



UNIVERSIDADE ESTADUAL DE CAMPINAS
SISTEMA DE BIBLIOTECAS DA UNICAMP
REPOSITÓRIO DA PRODUÇÃO CIENTÍFICA E INTELLECTUAL DA UNICAMP

Versão do arquivo anexado / Version of attached file:

Versão do Editor / Published Version

Mais informações no site da editora / Further information on publisher's website:

<http://www.sciencedirect.com/science/article/pii/S0895981115300092>

DOI: 10.1016/j.jsames.2015.06.002

Direitos autorais / Publisher's copyright statement:

©2015 by Elsevier. All rights reserved.

DIRETORIA DE TRATAMENTO DA INFORMAÇÃO

Cidade Universitária Zeferino Vaz Barão Geraldo

CEP 13083-970 – Campinas SP

Fone: (19) 3521-6493

<http://www.repositorio.unicamp.br>



Quartz sand resources in the Santa Maria Eterna formation, Bahia, Brazil: A geochemical and morphological study



Murilo Ferreira Marques dos Santos ^{a, *}, Eric Fujiwara ^b, Egont Alexandre Schenkel ^a, Jacinta Enzweiler ^c, Carlos Kenichi Suzuki ^a

^a Department of Materials Engineering, Faculty of Mechanical Engineering, Campinas State University (UNICAMP), Rua Mendeleiv, 200, Cidade Universitária Zeferino Vaz, Campinas, Brazil

^b Department of Integrated Systems, Faculty of Mechanical Engineering, Campinas State University (UNICAMP), Rua Mendeleiv, 200, Cidade Universitária Zeferino Vaz, Campinas, Brazil

^c Institute of Geosciences, State University of Campinas (UNICAMP), Rua João Pandiá Calógeras, 51, Cidade Universitária Zeferino Vaz, Campinas, Brazil

ARTICLE INFO

Article history:

Received 9 February 2015

Received in revised form

4 May 2015

Accepted 1 June 2015

Available online 4 June 2015

Keywords:

Quartz

Trace elements in quartz

Mineral resources

Silica glass

High purity quartz

ABSTRACT

This study presents an evaluation of the quartz sand occurrences of the *Santa Maria Eterna* formation, in northeastern Brazil, as a potential source of raw material for silica glass manufacturing. Samples of quartz sand were analyzed by ICP-MS to determine a range of trace elements and establish its chemical purity. The technological potential of the sand was obtained by counting the quantity of bubbles formed during flame fusion over silica plate. Both chemistry and bubble formation indicate that the raw material is suitable for producing silica glass. The work also investigated the composition of fluid inclusions in the quartz grains and the surface micro-texture by scanning electron microscopy. With the results obtained by these procedures, we inferred that the quartz sand was probably formed in a marine environment, by the precipitation of silica in the form of quartz. The main impurities of the samples are probably present in the mineral inclusions implying that purification is possible and probably competitive.

© 2015 Elsevier Ltd. All rights reserved.

1. Introduction

High purity quartz has been an important raw material for several industrial applications (Haus et al., 2012; Müller et al., 2012; Moore, 2005; Haus, 2005; Müller, 2007). It is used for the production of silica glass, a key material for high-end products, such as UV-lamps for purifying water (Barkhudarov et al., 2008; Wait et al., 2007); poly- and monocrystalline silicon solar cells, through its use as a material for crucibles (Gao et al., 2011; Kodama et al., 2010), and special devices with low thermal expansion. In order to be turned into a good quality silica glass, the quartz raw material must have unique characteristics. It must be pure, containing very low levels of metallic impurities such as Al, Fe and Ti, which can severely compromise the quality of the silica glass, jeopardizing its applications. Regarding the manufacturing of crucibles, Al excess can generate brown spots in the glass when it is in contact with the silicon melt and produce devitrification, reducing the lifetime of

the device, whereas Fe, Ti and other metallic impurities can contaminate the silicon melt (Minami et al., 2011; Yamahara et al., 2001; Huang et al., 1999). In the case of lenses and tubes, chemical impurities can affect the transmittance significantly, especially in the ultraviolet range (Schreiber et al., 2005; Kuzuu et al., 2003; Schultz, 1974).

Quartz for silica glass production must also contain low amounts of fluid inclusions. Such inclusions can produce bubbles during the fusion of the raw material into silica glass (Santos et al., 2013; Griscom, 2006). Usually, the amount of fluid inclusions in quartz is related to its opacity (Santos et al., 2013; Fujiwara et al., 2015), which can be used to grade the samples in order to obtain a better material quality.

Quartz resources with such characteristics are rare and their exploitation and processing are very costly (Santos et al., 2015; Suzuki et al., 2012; Haus et al., 2012; Götze, 2009). Often, companies start from less pure raw materials and use industrial processing to achieve the desired chemical purity. Such processing commonly involve acid leaching using HF and other hazardous materials (Li et al., 2010). The higher the amount of impurities in the raw material, the more expensive and environmentally damaging is the purifying process. Some chemical impurities, as Al,

* Corresponding author. Rua 3, n°2131, Rio Claro, São Paulo State, 13500-163, Brazil.

E-mail address: murilo@bmr.com.br (M.F.M. Santos).

Ti and Ge, substitute Si atoms in the quartz lattice and are much harder to be removed (Romanelli et al., 2012; Rakov, 2006; Götze et al., 2004), than Na, Ca and K that are often located in fluid inclusions (Götze, 2009). As a result, the chemical composition of the raw material, that is, the abundance and characteristics of its impurities, is a key factor in determining the economic potential of the quartz resource.

Extraction of the quartz raw material and its transformation into powder contributes significantly to the costs and, for this reason, sand constitutes as much cheaper and interesting resource than crystalline hard rocks. Brazil hosts many different kinds of quartz resources (Suzuki et al., 2012; Haus et al., 2012), many of them with a high degree of purity and favorable technological characteristics for silica glass production. However, most of the mines ascribed with high chemical purity, are rocky quartz deposits, but there are a number of quartz sand deposits as well. Most quartz sand deposits explored in the country are located in south and southeastern Brazil (Ruiz et al., 2013; Cruz, 2011) and are widely used by float glass manufacturers. Those resources, however, are not as pure as the rocky quartz deposits, what make them unattractive for silica glass manufacturers. They also contain large amounts of accessory minerals that are difficult to fully remove by industrial processing (Banza et al., 2006).

In this study, a newly discovered quartz sand deposit of economic potential, located in the state of Bahia, northeast Brazil, is described. Samples from the deposit were characterized by Inductively Coupled Plasma Mass Spectrometry (ICP-MS), fluid inclusion analysis, Scanning Electron Microscopy (SEM), cathodoluminescence and fusion over silica plate to document the chemical and physical properties of the raw material. This information were analyzed in order to evaluate whether or not the sand is fit for producing silica glass and to better understand its geological history.

2. Geology and petrology of the deposit

2.1. Geological setting

The deposit is located in a geological formation called *Formação Santa Maria Eterna*, in the south of the Bahia State, Brazil. This formation belongs to the *Rio Pardo* Group (Pedreira, 1999). The formation itself has not been precisely dated yet, but the age of other formations within the group were estimated as Neoproterozoic, between 800 and 500 Ma (Babinski, 2011; Pedreira, 1999). The maximum age of the *Rio Pardo* group is reported to be about 1.0 and 1.1 Ga, according to measurements on basal basaltic pebbles located within the *Panelinha* conglomerate (Teixeira et al., 1997; Karmann, 1987).

The *Santa Maria Eterna* formation is situated southwest to the city of Belmonte. The formation crops out in an area of approximately 30 times 20 km as shown in Fig. 1 (Babinski, 2011). The mine is located in the central part of the area. The formation consists almost exclusively of quartz sand and minor quantities of quartz pebbles up to 20 cm. Conglomerates and carbonatic intercalation with tepee structures are also found in the formation (Cezario et al., 2011). The surrounding formation within the *Rio Pardo* Group, called *Serra do Paraíso* formation, comprises carbonate rocks with stromatolites and quartzites (Babinski, 2011; Cezario et al., 2011; Karmann, 1987). It is generally accepted that both the *Serra do Paraíso* and the *Santa Maria Eterna* formations were deposited over the *Panelinha* conglomerate in a marine environment (Babinski, 2011). A more detailed description of the geological setting of the formation is found in the above cited literature.

The deposit itself is not being commercially exploited. There are, however, projects for using the sand in the manufacture of special glasses and mining activities may start within the next few years.

2.2. Petrography

The deposit is composed of highly homogeneous white-colored sand. The sand is covered by black soil containing burned organic matter. The organic layer is approximately 20 cm thick and, immediately below it, occurs a layer of yellow clay. The clay layer is usually less than a meter in thickness. Fig. 2 displays an image of the outcrop. Other layers, composed of red and yellow (in the web version) clays up to 15 cm thick, can be developed at greater depths. Below these depths, pure quartz sand occurs to a depth to 30 m.

The sand is presented as gravel. No sandstone or agglomeration of quartz grains were present. An estimation of the particle size distribution was made by sieving. The higher amount, about 80%–85% of the particles passed through the 35 mesh sieve (Tyler scale, with an opening of 0.5 mm) and was retained in the 80 mesh sieve (with an opening of 0.18 mm). Larger particles, i. e., retained in the 35 mesh sieve, contributed in average for 15–19% of the total amount. Smaller particles contributed for 2–3%. The shape of the particles were mainly irregular. The general aspect of the sand can be seen in Fig. 3.

The quartz sand contains a few brownish spots, probably Fe-bearing accessory minerals. Fig. 4 shows one of these spots. The brown (in the web version) material is trapped within an aggregate of smaller quartz grains, and has no apparent crystal habit. X-ray diffraction analysis of the bulk sand, displayed in Fig. 5, can confirm the lack of crystallinity (or the extremely small concentration) of the Fe-bearing impurity, since no other peaks than those of the α -phase of quartz are developed. The SEM-EDX analysis of the spot revealed a significant Fe concentration.

A detailed description of the fluid and melt inclusion inventory of quartz grains in the sand is provided in the result chapter.

3. Analytical methods and characterization of technological (physicochemical) properties

3.1. Fluid inclusion observation using optical microscopy

For the fluid inclusion observation, a small amount of sand was placed on a microscope slide. In order to improve the observation of the sand grains, a film of kerosene was applied over the sand. The kerosene has a refractive index similar of that of the silica, which reduces undesired surface observation.

A Nikon optical microscope operated at 500 × magnification was used to acquire transmitted light photographs for fluid inclusion analysis, using a Nikon digital camera. All photographs were taken at room temperature.

Using this methodology, it was possible to obtain insights on the nature of the fluid and mineral inclusions present in the sand. Although a more complete analysis were not carried on, regarding homogenization temperature and other key properties of the inclusions, it was possible to obtain good quality data on mineral inclusions. This data was vital in order to reconstruct the genetic conditions of the mineral.

3.2. Chemical analysis using inductively coupled plasma mass spectroscopy (ICP-MS)

For the chemical purity evaluation, eight samples were collected from the mine. The samples were distant to each other at least 10 m, to evaluate the variability of the chemistry within the deposit. All samples presented the same visual aspect, consisting of white sand with eventual black spots. The samples were collected using a drill at a depth of about 2 m. This procedure avoided the upper parts of the deposit, i. e., the black organic matter layer and the yellowish sand layer. About 300 g of sand was collected in each site.

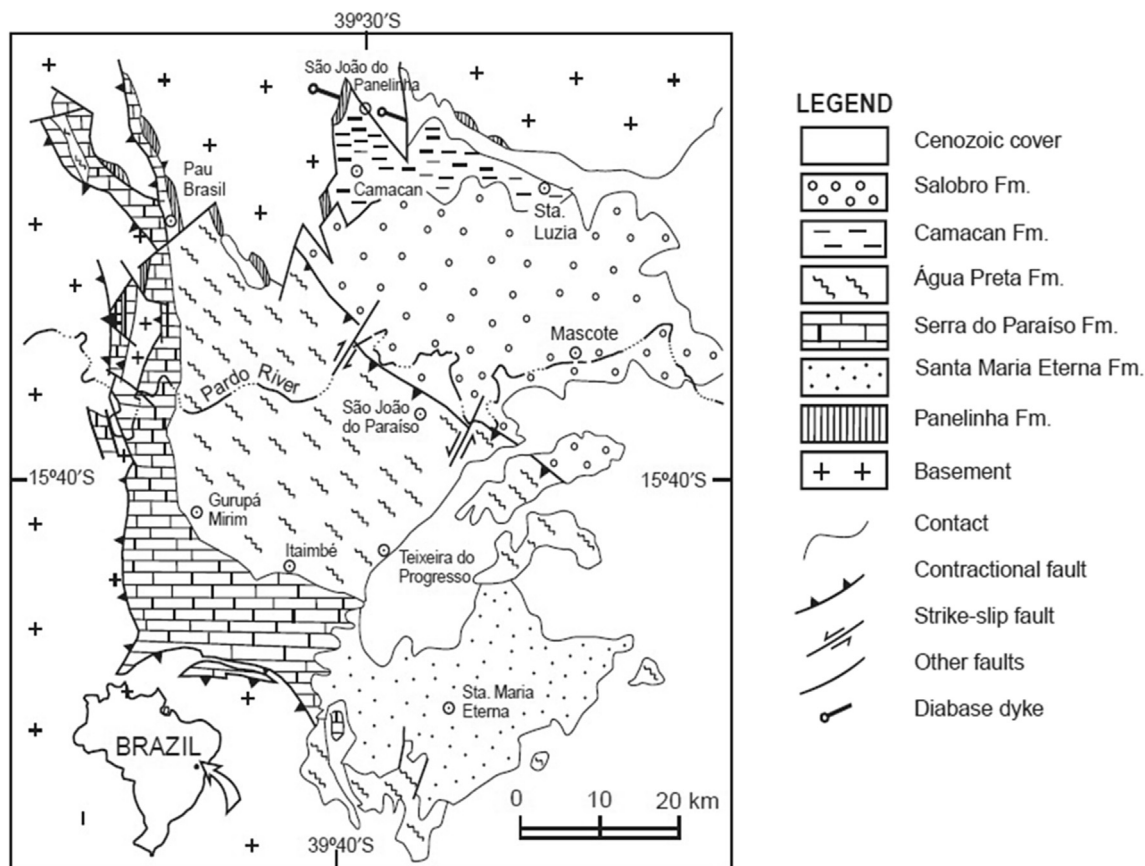


Fig. 1. Geological map of the studied area showing the position of the Santa Maria Eterna formation and its neighboring formations according to Babinski (2011).

Each sand sample was washed with distilled and deionized water, and dried and crushed in a silica glass mortar, in order to avoid contamination. The crushed powder was sieved with a 500 mesh nylon sieve, to guarantee that the particles were smaller than 25 μm .

Test portions of 100 mg were weighed and digested in perfluoroalkoxy vessels (PFA, Savillex, USA) by adding 0.5 mL of purified HF and heated at 80 °C for 1 h, followed by evaporation to dryness at 120 °C. After cooling to room temperature, 0.5 mL of HF

and 0.1 mL of distilled HNO_3 were added to the vessels, which were closed with their lids and kept at 110 °C for 24 h. The vessels were allowed to cool, opened and acid was evaporated. The residue was recovered in 0.5 mL HNO_3 and transferred into polypropylene tubes where the solution was brought to 10.0 g by adding ultrapure water.

All procedures were conducted in a clean room laboratory and all acids were purified by sub boiling. The water was obtained after ion exchange and reverse osmosis (Milli-Q, Millipore). The measurements used an ICP-MS instrument X Series II (Thermo, Germany) equipped with Collision Cell Technology (CCT). The instrument was calibrated using solutions of certified reference materials diluted accordingly. Signal drift was monitored and corrected by adding In and Re as internal standards. The accuracy of the measurements was confirmed by analysis of reference material BCS-CRM 313/1 and details can be verified elsewhere (Santos et al., 2014).

3.3. Morphology and micro texture analysis of the sand using scanning electron microscopy (SEM)

The morphology and micro texture of the sand particles can provide valuable information on the geological history of the deposit (Vos et al., 2014). This kind of analysis is often conducted using scanning electron microscopy (SEM) due to the ability of this technique to identify a wide range of textural features of different sizes. However, the results are very dependable on the sample preparation. Vos et al. (2014) reviews sample preparation procedures that mostly consist in removing other minerals or substances that might be adhered to the surface of the particles.

For this work, samples were prepared by selecting a clean portion of one of the samples, which was washed in distilled and



Fig. 2. Image of the sand outcrop (upper part of the photo).

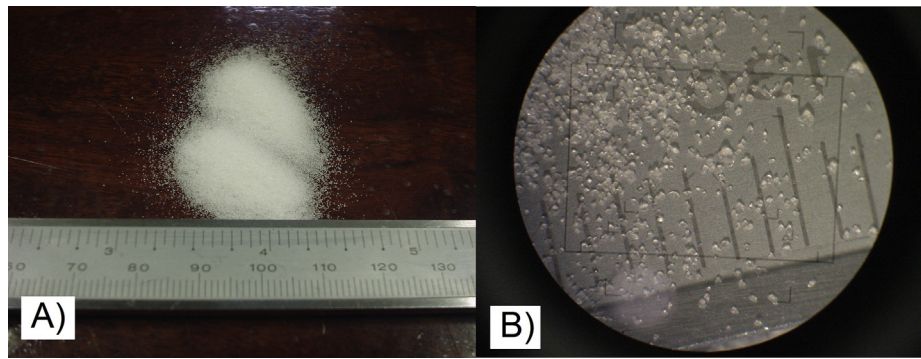


Fig. 3. Overall aspect of the sand. A) shows the material as it is in nature, as gravel, and B) shows the gravel in a low magnification photograph.



Fig. 4. Photograph of a black spot present in the bulk sand. It can be seen that the black spot is an agglomerate of small quartz grains stuck at a Fe-bearing grain.

deionized water. Acid treatment tests were performed with HCl and HNO₃. HF was avoided once it could cause mass loss and artificial structures on quartz grains. No differences in texture were observed when comparing the sample only cleaned with water and those immersed in HCl or HNO₃ at 80 °C for 6 h. Therefore, the simple ultrapure water washing procedure was adopted. The clean sand particles were transferred to a steel stub and covered with a gold thin film by sputtering in a vacuum chamber.

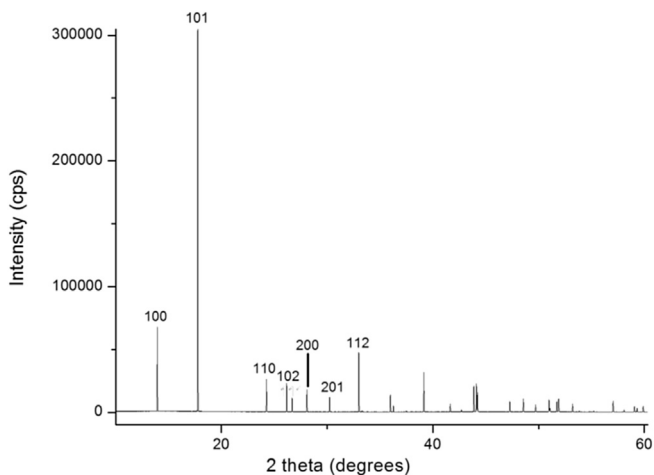


Fig. 5. High resolution X-ray diffraction pattern of the bulk sand, collected using a synchrotron radiation source of 12 keV. Only peaks of alpha-quartz were registered.

The analysis were performed on a SEM Zeiss instrument, model EVO MA15, equipped with a thermo ionic LaB₆ electron source. Images were obtained on a secondary electron detector, with a biased grid of 250 V. The acceleration voltage is given on the images.

3.4. Scanning electron microscopy cathodoluminescence (SEM-CL) analysis

For the cathodoluminescence analysis it was used a Zeiss Company scanning electron microscope, model LEO 430i equipped with a GATAN Chroma CL cathodoluminescence detector. The microscope operated with a 10 keV acceleration voltage.

The sample preparation consisted in separating small amounts of sand that were embedded in thermoplastic resins. After the cure of the resin, the system (resin and sand) was submitted to optical polishing using cerium oxide and diamond paste. After polishing, the sample was coated with C using a Quorum Technology sputter equipment, model Q150T.

3.5. Fusion over silica plate

A small portion of fine sample powder was placed over a silica plate and fused by blowing a H₂/O₂ torch above it. As the particles melt, their fluid inclusions grow into stable bubbles. The size of those depends on several factors. As a result it is possible to estimate the powder's response during the industrial processes. Several silica glass manufacturers use this simple essay to evaluate the potential of a quartz powder to produce glass (Torikai, 1994).

In this work, as the sand already has a particle size suitable to most fusion powders, i. e., between 75 and 180 μm, no sieving or crushing was required. The fusion parameters, as the torch distance to the plate and the fusion time were kept at about 4 mm and 15 s, respectively, although minor fluctuations may have occurred. The torch stoichiometry was also controlled and kept constant.

4. Results

4.1. Fluid and mineral inclusions

Examples of the observed fluid and mineral inclusions are shown in Fig. 6, to 9. Several inclusion types can be observed.

A common fluid inclusion morphology observed in several grains is the negative hexagonal crystal-shaped inclusion, with a gas bubble occupying 40–80% of the inclusion volume (shown on Fig. 6). This is a very common shape for fluid inclusions in quartz (Santos et al., 2014; Götze, 2009; Van der Kerkhoff and Hein, 2001; Roedder, 1984).

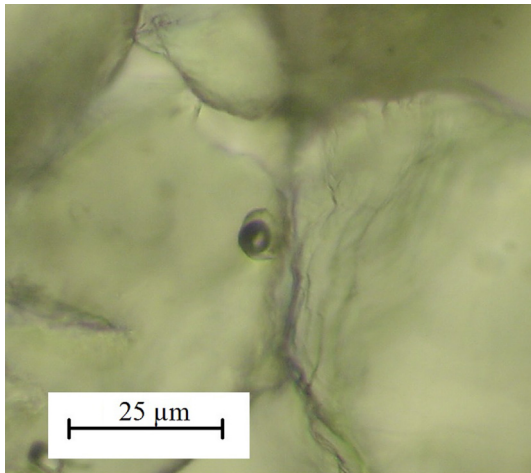


Fig. 6. Photograph of the quartz grains. The fluid inclusion has a negative crystal-shaped fluid inclusion and contain a large gas bubble.

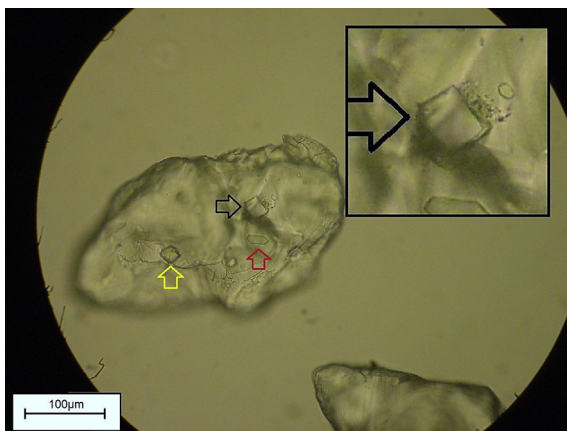


Fig. 7. Photograph of the inclusions on the quartz sand grains. The red arrow indicates an apatite mineral inclusion. The black arrow indicates a rhombohedral crystal inclusion. A cluster of smaller inclusions beside the rhombohedral inclusion can be observed indicating paleo-decryption. The detail shows a magnified image of the rhombohedral inclusion. The yellow arrow indicates a dypiramidal inclusion. (For interpretation of the references to colour in this figure legend, the reader is referred to the web version of this article.)

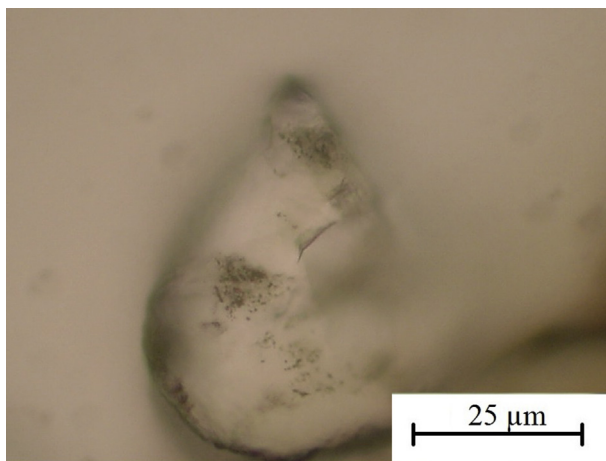


Fig. 8. Photograph of the cluster shaped fluid inclusions. This kind of inclusion consists of a group of apparently spherical monophasic inclusions.

Another observed morphological features were the crystal like shaped inclusions, as seen in Fig. 7. These kind of inclusion is related to presence of mineral inclusions in quartz. When the other minerals crystallize within the quartz, it can induce the generation of several shapes of crystals within the mineral. In the analyzed samples, we could observe several mineral inclusions with different shapes. Some of them are the rhombohedral inclusions containing a visible liquid phase, as indicated by the black arrow in Fig. 7. We suggest that those crystals, possibly calcite, were probably formed in the presence of saline fluids. In Figs. 7 and 9, we can also notice the presence of orthorhombic dypiramidal (yellow arrow in Fig. 7) and hexagonal dypiramidal (Fig. 9 and the red arrow in Fig. 7) (in the web version) crystals. The later was further analyzed by cathodoluminescence (Fig. 9) and presents a clear purple luminescence, indicating that it is probably an apatite crystal (Kempe and Götze, 2002). A correlation of these morphological features and the chemical composition of the quartz is discussed below.

The sample also presented “cluster shaped” minute inclusions as shown in Fig. 8. These clusters differ from the inclusions Fig. 7 (to be commented) once they are not satellites of larger inclusions. Because the individual inclusions were smaller than the resolution of the optical microscope, precise information concerning their shape and composition could not be obtained. Due to this difficulty, we cannot state if they are mineral or fluid inclusions.

Fluid or mineral inclusions were observed in all sand particles, yet more than 50% of them had at least one large inclusion. This feature has relevant technological implications because larger inclusions commonly produce bubbles during quartz melting. Table 1 summarizes the most common types of inclusions present in the sample and estimates their frequency.

4.2. Morphology and micro-texture analysis by SEM technique

The SEM images of the studied sand samples are shown in Fig. 10, to 12. In these figures, a characteristic feature is recognizable on the surface of the sand particles. It consists of parallel growth lines of tiny (2–4 μm) subcrystals (Fig. 10, detail in Fig. 11) suggestively grown under diagenetic or authigenic conditions (Vos et al., 2014; Kelly et al., 2007; Waugh, 1970). This authigenic hypothesis is coherent with the different types of fluid inclusions observed, and will be further discussed below.

The shape of the grains is also notably homogeneous, showing irregular shapes and the negative crystal-shaped inclusions emerging on the surface. On several grains, typical conchoidal marks (Fig. 12a) and etch-pits (Fig. 12b) can be observed. According to Vos et al. (2014) etch-pits are produced by local dissolution of quartz within mineral solution. Krinsley and Doornkamp (1973) relate these pits to etching in slightly basic (pH around 7 or 8) environments. Such pH characteristics could be found in marine environments. Conchoidal marks can be produced by high pressure during rock formation, as in glacial deposits (Mahaney, 2002), or by fractures near mineral inclusions that weaken the crystal (Le Ribault, 1977). Impacts during transport and sedimentation can also cause such marks (Vos et al., 2014), especially in marine environments. One can also observe that the crystal overgrowths in Fig. 11 are mildly rounded, which can also be an evidence for marine deposition.

4.3. Chemical analysis using inductively coupled plasma mass spectroscopy (ICP-MS)

Table 2 presents the trace elements content in the sand samples from the Santa Maria Eterna formation. For comparison the same table has the values of Müller et al., 2007 for the same elements in

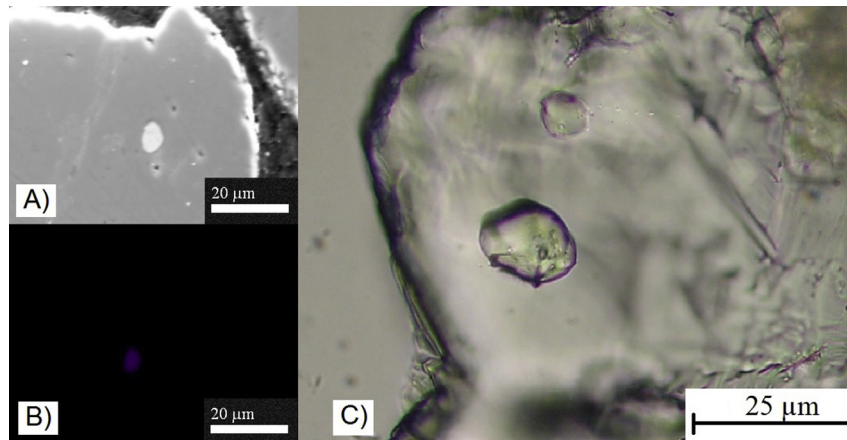


Fig. 9. Photograph (C), SEM secondary electrons (A) and cathodoluminescence (B) of the hexagonal dipyramidal mineral inclusions. The purple cathodoluminescence and the shape suggest that those are apatite crystals. (For interpretation of the references to colour in this figure legend, the reader is referred to the web version of this article.)

Table 1
Most common types of inclusions, their size and frequency estimation.

Type	Displayed in	Size (μm)	Frequency
Biphasic negative hexagonal crystal	Fig. 6	from 2 to 10	Present in about 5% of the grains
Hexagonal dipyramidal crystal	Figs. 9 and 7 (red arrow)	from 1 to 20	Present in about 15% of the grains
Rhombohedral crystal	Fig. 7 (black arrow)	from 1 to 25	Present in about 20% of the grains
Non-hexagonal dipyramidal crystals	Fig. 7 (yellow arrow)	from 5 to 10	Present in about 5% of the grains
Cluster-like inclusions	Fig. 8	below 1	Present in about 30% of the grains

the commercial high purity quartz powders Iota (Unimin Corporation) and Drag (Norwegian Crystallites AS).

The elements listed in Table 2 represent more than 95% of the trace elements present in the samples. Other elements also evaluated (Ag, Ba, Be, Ce, Co, Cs, Dy, Er, Eu, Ga, Hf, Ho, La, Lu, Nb, Nd, Ni, Pb, Pr, Rb, Sb, Sc, Sm, Sn, Ta, Tb, Te, Th, Tl, Tm, U, V, W and Y), but their values were very low and were omitted. Li, Zr and B also presented low values but were not omitted due to their significance in quartz technology (Götze, 2009).

Table 2 shows that all the samples have a similar composition. The main contaminants consisted of Ca (ca. $150 \mu\text{g g}^{-1}$) followed by Mg (ca. $41 \mu\text{g g}^{-1}$). The Ca/Mg ratio varied between from 2.7 to 4.8.

Ca and Mg in quartz are commonly associated to mineral inclusions (Götze, 2012, 2009; Götze et al., 2004). Such relatively high amounts of Ca and Mg are also found in quartz of sandstones formed in saline environments (Götze, 2012; Fruth and Blankenburg, 1992). They result as the crystallization of Mg and Ca chlorides, present in the surrounding fluids.

The Al content, however, presents an abnormally low value. Most quartz resources, either hydrothermal, pegmatitic or diagenetic, usually contain more than $20 \mu\text{g g}^{-1}$ in Al (Santos et al., 2014; Götze, 2012; Müller et al., 2012; Suzuki et al., 2012; Li et al., 2010; Müller et al., 2007; Iwasaki et al., 1991). The content of Ge is also relatively low. These two trace elements are important substituents of Si in the quartz crystalline structure, along with Ti that will be

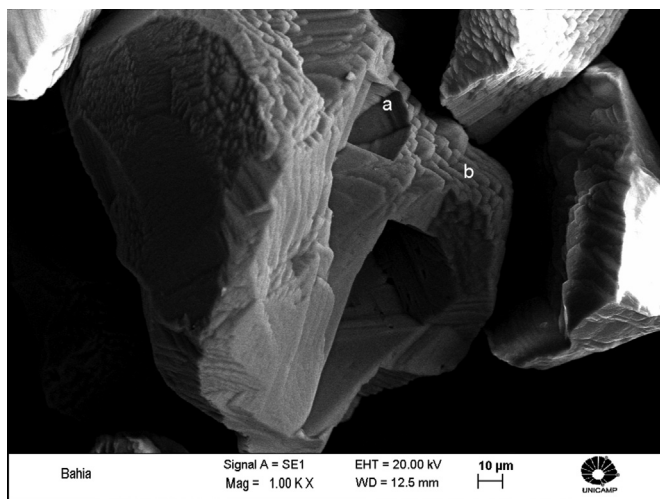


Fig. 10. SEM image showing the surface of irregular quartz grains. The surfaces are coated with line-like arranged quartz sub-crystals presumably of authigenic origin (b). Occasionally negative quartz crystal shapes are developed (a).

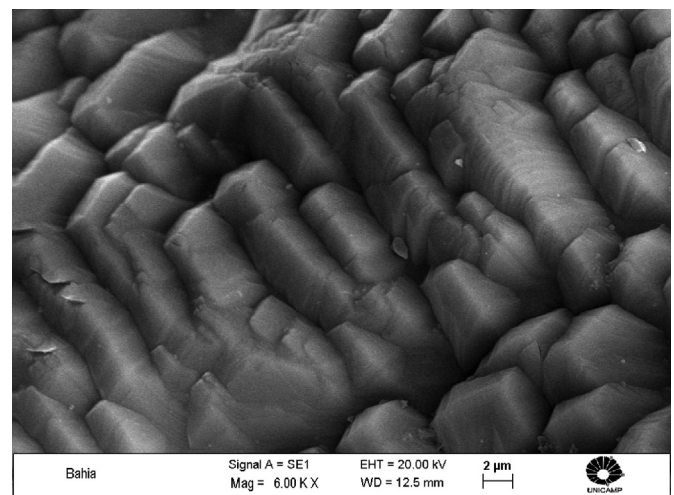


Fig. 11. Detail of the quartz overgrowth of the sand grains of the Santa Maria Eterna formation.

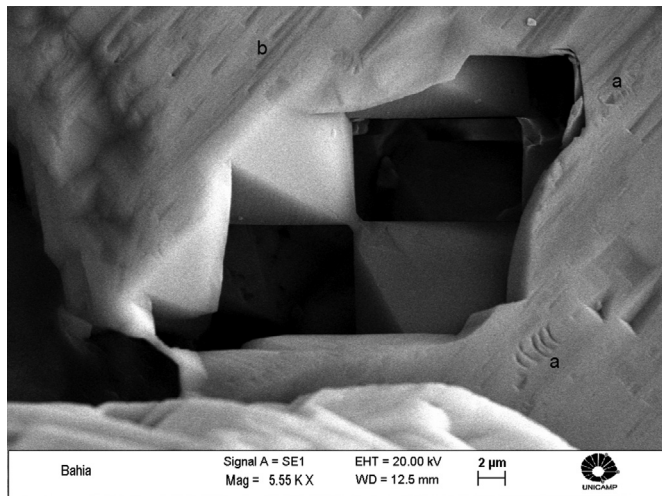


Fig. 12. Image of textures in the quartz grain surfaces. At a) conchoidal marks and at b) triangular etch pits can be observed.

commented further in the text, (Romanelli et al., 2012; Rakov, 2006; Götze et al., 2004). Their low values is in line with the low concentration in K and Li, which are charge compensators for Al^{3+} defects. The Al/Li ratio is larger than 60 for all samples, attaining 99 in sample 5. This implies that either the Al is not a substituting impurity, what is very unlikely considering the very low Al content, or that the fluid was very poor in Li, and the charge unbalance was compensated by other ions. However, the K and Na content are also relatively low. A possible alternative for the charge unbalance compensation is H^+ (Müller et al., 2012; Müller and Koch-Müller, 2009; Müller et al., 2003), the last not being able to be detected by ICP-MS (Romanelli et al., 2012; Götze, 2009). This kind of charge compensation tends to happen the mineral crystalizes in a wet environment, as in hydrothermal quartz samples or precipitation in marine environments. This suggests that a marine genesis is a plausible explanation for most of the quartz present in the *Santa Maria Eterna* formation.

All samples contain other metallic trace elements, such as Cu, Fe, Ti and Zn in amounts higher than $1 \mu g g^{-1}$. The amount of Fe and Ti is little higher. These latter elements are common in quartz samples, but they can be in the accessory minerals, as the black grains, aforementioned. Samples 7 and 8 contain higher values of Fe, Cu and Zn suggesting the presence of non-lattice impurities. The Ge/Fe ratio, used to discriminate the genetic origin of quartz by Götze et al. (2004) and Schrön et al. (1982), is lower than 0.1 for all

samples. Often, pegmatitic quartz and hydrothermal quartz formed at higher temperatures can present a high Ge content (Götze et al., 2004). Although part of the Fe in the studied samples may not be in the quartz, the Ge content is very low. Even by assuming that all Fe is bound in accessory minerals, the Ge/Fe would be too low to exclude a hydrothermal origin of the observed quartz overgrowth. In more than 500 g sand, only 3 or 4 black grains were observed. The geochemistry of the samples will be further discussed below.

4.4. Scanning electron microscopy cathodoluminescence analysis (SEM-CL)

The quartz sand presented only a faint reddish cathodoluminescence, as it can be seen on Fig. 13. The mineral inclusions presented in the samples presented a much more intense luminescence. This faint red luminescence is often present in authigenic quartz and hydrothermal quartz (Götze et al., 2001). The emission is attributed to the recombination of electrons in the non-bridging oxygen band-gaps. Götze et al. (2001) also states that impurities such as silanol (Si–OH) groups and H^+ impurities could act as precursors for these non-bridging oxygen defects. This red luminescence adds evidence to the hypothesis that the Al defect centers are indeed being charge compensated by H^+ ions.

Another interesting fact observed in Fig. 13 is the absence of distinct luminescence zones in the grains. This suggests that the overgrowth patterns were not grown over detrital quartz sands, as it happens in most diagenetic quartz. It seems more likely that the grains and the observed pattern were formed in the same crystallization event.

4.5. Fusion over silica plate

Fig. 14 shows three tests of sand samples and one of IOTA commercial powder after fusion over a silica plate. All tests present a similar aspect regarding bubble formation. The size and amount of bubbles vary among the samples. The sample shown in Fig. 14a contains much more and larger bubbles than the sample shown in Fig. 14c which contains only a few bubbles. The latter has a similar proportion of bubbles as found in the fused Iota sample (Fig. 14d)."

The formation of bubbles can be related to the presence of fluid inclusions in quartz grains. If these contain a large volume of fluid inclusion gases, the production of large bubbles during fusion can be expected. Inclusions as shown in Fig. 6 will generate bubbles as those in Fig. 14a. Smaller inclusions might as well produce bubbles, but they will be smaller, as those in Fig. 14c. Grains without fluid inclusions will generate silica glass free of bubbles.

Table 2

Trace elements concentrations of samples from Santa Maria Eterna formation and of some commercial high purity quartz powders.

Sample	Al	B	Ca	Cr	Cu	Fe	Ge	K	Li	Mg	Mn	Na	Ti	Zn	Zr
Impurity content ($\mu g g^{-1}$)															
Sample 1	7.5	<0.8	147	0.04	1.8	4.2	0.37	<5	<0.1	42	<0.1	<7	3.9	1.3	<0.2
Sample 2	6.9	<0.8	148	0.03	1.3	3.6	0.34	<5	<0.1	41	<0.1	<7	3.4	1.1	<0.2
Sample 3	8.3	0.8	144	0.03	2.6	3.6	0.36	<5	<0.1	50	<0.1	<7	4.1	1.3	<0.2
Sample 4	7.2	<0.8	161	0.02	2.1	4.1	0.37	<5	<0.1	47	<0.1	<7	5.3	1.2	<0.2
Sample 5	9.9	0.9	145	0.03	2.8	3.9	0.36	<5	<0.1	53	<0.1	<7	5.5	1.4	<0.2
Sample 6	8.4	<0.8	161	0.02	3.6	3.5	0.37	<5	<0.1	33	<0.1	<7	4.2	1.3	<0.2
Sample 7	7.6	<0.8	144	0.04	5.4	12.4	0.34	<5	<0.1	30	<0.1	<7	4.8	4.3	<0.2
Sample 8	7.5	<0.8	151	0.04	6.1	8.2	0.36	<5	<0.1	32	<0.1	<7	4.4	4.7	<0.2
Commercial quartz powders (Müller et al., 2007)															
Iota STD	16.2	0.08	0.5	n.a.	n.a.	0.2	n.a.	0.6	0.9	n.a.	<0.05	0.9	1.3	n.a.	n.a.
Iota 8	7	<0.08	0.5	n.a.	n.a.	<0.03	n.a.	<0.04	<0.02	n.a.	<0.02	0.03	1.2	n.a.	n.a.
Drag NC1	26	<0.4	0.6	n.a.	n.a.	0.5	n.a.	0.7	4	n.a.	0.01	2.7	4.0	n.a.	n.a.
Drag NCA	7	n.a.	0.1	n.a.	n.a.	0.1	n.a.	0.3	0.7	n.a.	<0.01	0.7	4.0	n.a.	n.a.

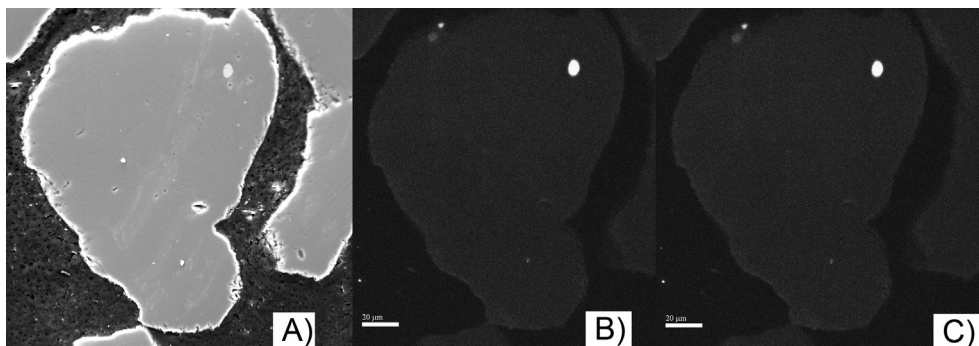


Fig. 13. SE–SEM image of the grain (A), red cathodoluminescence signal (B) and the sum of red, green and blue luminescence (C). The cathodoluminescence shows no zoning in the quartz grains, indicating one single crystallization event.

5. Discussion

5.1. Technological aspects

The economic viability of the quartz sand deposit of *Santa Maria Eterna* formation as raw material to produce silica glass depends on its chemical composition and propensity to form bubbles. Beside the chemical composition and fluid inclusion content, the possibility to purify the starting raw resource to improve its quality must also be considered.

Table 2 compiles the main impurities of commercial powders. Full references of high quality raw material can be found in Santos et al. (2014), Suzuki et al. (2012), Beurlen et al. (2011), and Iwasaki et al. (1991) for Brazilian quartz; Müller et al. (2012, 2007, 2003) for Norwegian quartz; and Götze (2009) and Götze et al. (2004) for quartz from different countries. The comparison of quartz from *Santa Maria Eterna* to other sources of high purity quartz described in literature, shows that the studied sand has a very low Al content as it is found in nature. The average Al content of $7.5 \mu\text{g g}^{-1}$ is

similar to that of the commercial powders, and even lower than Iota STD or Drag NC1. Al is stated as the most difficult element to remove, because it substitutes Si in the crystalline structure. Often, significant purification can be only achieved using HF or concentrated acid mixtures, which is environmentally hazardous and expensive (Du et al., 2011; Li et al., 2010; Lee et al., 2006; Liu et al., 1996; Ubaldini et al., 1996).

Ca and Mg are the only problematic impurities, once their contents in the material are very above that of the commercial powders. As already mentioned, the concentration of these constituents can be related to the high content of chlorides in precursor fluid (Götze et al., 2012). These impurities may be located mostly in the fluid inclusions, as high-saline brines, or as mineral inclusions in the grains. This last hypothesis is highly probable because optical observation and SEM detected several mineral inclusions (as apatite). The same possibly applies to the Na and K impurities.

Some industrial processing procedures allow the removal of fluid and mineral inclusions. Examples are heat treatments (Haus et al., 2012), electrical fragmentation (Dal Martello et al., 2011)

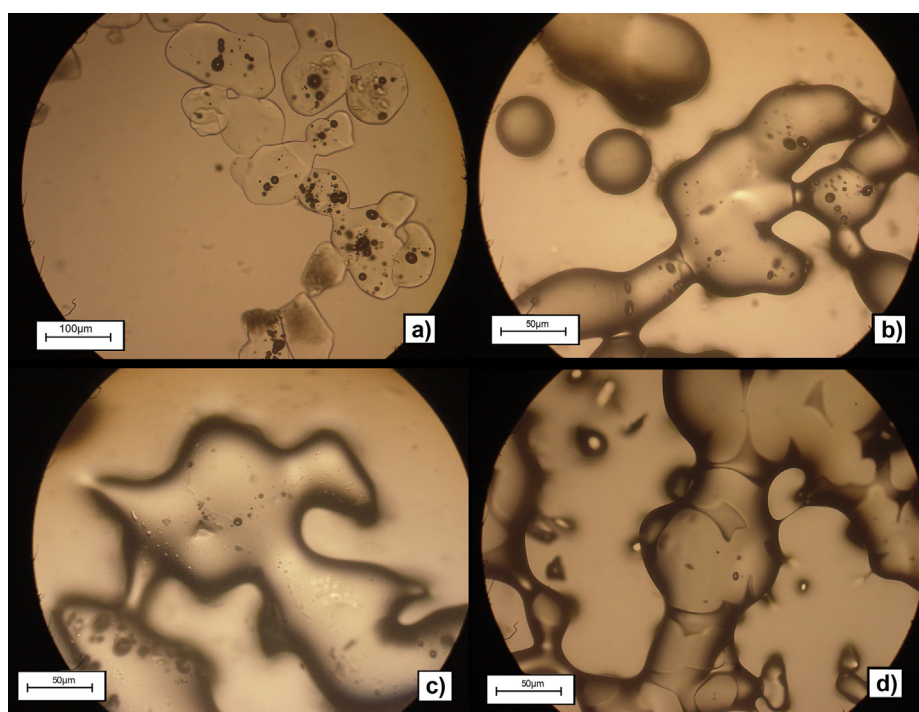


Fig. 14. Photographs with aspect of three test a), b) and c) of sand and of d) lota quartz commercial powder after fusion over silica plate.

and radiation methods (Belashev and Skamnitckaya, 2009). Once the inclusions are fragmented, washing the samples with distilled and deionized water could remove chemical impurities. Dilute acids can also be used as cleaning agents, dissolving mineral inclusions selectively. These treatments can improve both the chemistry and the quality of fused products, by avoiding the generation of bubbles. With these treatments, the bubbles observed in the silica plate fusion test would probably be less both in size and number.

Metallic impurities (Fe, Ti, Cu and Zn) can be significantly removed by acid leaching with dilute oxalic, sulfuric or hydrochloric acids, and as proposed by several authors for poor quality raw materials, as long as these impurities are not on substitutional positions (Du et al., 2011; Li et al., 2010; Lee et al., 2006; Banza et al., 2006). Overall, the chemical composition of the sand in the *Santa Maria Eterna* formation makes it a valuable resource. Probably it could be purified to become a commercial high purity quartz source to produce a good and clean transparent glass.

Nevertheless, the studied material can be used as a raw material in the silica glass industry to obtain opaque crucibles without the proposed treatments. Examples of crucibles used in silicon purification, made from silica containing larger amount of impurities than the mainstream commercial powders (IOTA, Drag, etc.), can be found in the literature. For instance, Kvande et al. (2009), Dhamrin et al. (2009) and Yamahara et al. (2001) produced quartz crucibles with more than $5 \mu\text{g g}^{-1}$ Fe and $6 \mu\text{g g}^{-1}$ Ti.

5.2. Geochemistry, morphology and geological history

The data also provide some insights on the genesis of the quartz in the *Santa Maria Eterna* formation. The surface morphology shows patterns (Figs. 10 and 11) of crystalline overgrowth, when analyzed together with the cathodoluminescence images (Fig. 13) indicates an authigenic crystallization (Vos et al., 2014; Madhavaraju et al., 2006). Such pattern is often due to precipitation of silica from silica-rich fluids in conditions that allow quartz crystallization.

This authigenic marine hypothesis is especially interesting when we regard the geological setting of the area and the mineral inclusions in the sample. The neighboring Serra do Paraíso formation has carbonates with stromatolites (Babinski, 2011; Cezario et al., 2011; Karmann, 1987), suggesting a marine environment. Karmann (1987) and Babinski (2011) propose that the *Santa Maria Eterna* formation itself was formed in a marine environment. The presence of apatite crystals as mineral inclusions also points towards a direct mineralization from the sea.

The geochemical composition of the quartz also corroborates with such hypothesis. The data of Table 2, show relatively high amounts of Ca and Mg (up to $200 \mu\text{g g}^{-1}$ in some samples). These unusual values in quartz, are reported in authigenic quartz from marine environments (Götze et al., 2012, 2004; Kempe et al., 2012; Fruth and Blankenburg, 1992). Some marine environments can precipitate silica when the water is rich in CaCl_2 and MgCl_2 . Several works state that a marine environment with such characteristics would precipitate, along with apatite, calcite, aragonite or Mg-rich calcite (Schmidt et al., 2005; Jiménez-López, 2004; Goldstein, 2001; Alexandersson, 1972). The presence of such minerals would explain the rhombohedral and orthorhombic mineral inclusions present in Fig. 7.

The evidences indicate that the quartz in the *Santa Maria Eterna* indeed precipitated from a marine environment. A probable cause of the precipitation could be changes in the temperature or pressure of the water in which the silica was dissolved or even a sudden increase in the CaCl_2 and MgCl_2 concentrations in the silica-saturated ocean. These salts are known to decrease silica solubility in water even at small concentrations (Barker et al., 1994; Chen

and Marshall, 1982). This could explain the preferential formation of quartz, instead of dolomite, calcite or aragonite.

Once formed, the quartz deposited. This could explain the absence of transport marks other than the few conchoidal fractures observed by SEM. The increased salinity of the ocean and the presence of chlorides could also explain the etch marks present in Fig. 12.

An open question is the source of silica in this ancient ocean. One possibility is the dissolution of amorphous silica of biological origin and its recrystallization as reported in several other environments (Loucaides et al., 2012; Schieber et al., 2000).

6. Conclusion

The high purity quartz sand of *Santa Maria Eterna* formation is a promising ore resource. It was probably formed by silica precipitation from a marine environment, generating an ore with very low Al and high Mg and Ca contents, contained mostly in mineral inclusion. Very few accessory minerals (other than mineral inclusions) are found in the deposit and it is also remarkably homogeneous.

Its viability as raw material for silica glass production showed adequacy for several applications. The quartz sand is sufficiently pure and the product of fusion has little number of bubbles. Moreover, as the main impurities are in fluid and mineral inclusions, they could be removed by purification. The resulting powder could become a competitive product in the high purity quartz market.

Acknowledgements

The authors acknowledge scholarships and funding from Brazilian agencies CAPES, National Council for Scientific and Technological Development - CNPq and São Paulo Research Foundation - FAPESP. The Brazilian Synchrotron Light Laboratory (LNLS) is acknowledged for the synchrotron high resolution X-ray diffraction data.

The authors are grateful to the companies BMRC Mineral Technology (*Beneficiamento de Minérios Rio Claro Ltda*) for financial and scientific support, and Silica Del Piero for prospecting the quartz deposit. From the last company, engineers Jorge Teixeira and Antonio Gil deserve especial gratitude for fieldwork support.

References

- Alexandersson, T., 1972. Intergranular growth of marine aragonite and Mg-calcite: evidence of precipitation from supersaturated seawater. *J. Sediment. Petrology* 42, 441–460.
- Babinski, M., 2011. Geocronologia das Glaciações Criogênicas do Brasil Central. Habilitation Thesis. Universidade de São Paulo, p. 190 (in portuguese).
- Barker, P., Fontes, J.-C., Gasse, F., Druart, J.-C., 1994. Experimental dissolution of diatom silica in concentrated salt solutions and implications for paleoenvironmental reconstruction. *Limnol. Oceanogr.* 39 (1), 99–110.
- Barkhudarov, E.M., Christofi, N., Kossyi, I.A., Misakyan, M.A., Sharp, J., Taktakishvili, I.M., 2008. Killing bacteria present on surfaces in films or in droplets using microwave UV lamps. *World J. Microbiol. Biotech.* 24, 761–769.
- Banza, A.N., Quindt, J., Gock, E., 2006. Improvements of the quartz sand processing at Hohenbocka. *Int. J. Miner. Process.* 79, 76–82.
- Belashev, B.Z., Skamnitckaya, L.S., 2009. Irradiation methods for removal of fluid inclusion from minerals. *RMZ- Minerals Geoenvironment* 56, 138–147.
- Beurlen, H., Müller, A., Silva, D., Da Silva, M.R.R., 2011. Petrogenic significance of trace-element data analyzed with LA-ICP-MS in quartz from the Borborema pegmatitic province, northeastern Brazil. *Mineral. Mag.* 75, 2703–2719.
- Cezario, W.S., Sial, A.N., Misi, A., Pedreira, A.J., Gaucher, C., Ferreira, V.P., Lacerda, L.D., 2011. Carbon-isotope and Hg stratigraphies of the neoproterozoic serra do paraíso (Rio pardo Basin) and são Desidério (Rio Preto Belt) formations, bahia, Brazil. In: XIII Congresso Brasileiro de Geoquímica, Gramado, pp. 1163–1166.
- Chen, C.-T.A., Marshall, W.L., 1982. Amorphous silica solubilities IV: behavior in pure water and aqueous sodium chloride, sodium sulfate, magnesium chloride and magnesium sulfate up to 350°C. *Geochimica Cosmochimica Acta* 46 (2), 279–287.

- Cruz, T.T., 2011. Caracterização de depósitos de areia da bacia sedimentar de Taubaté para a fabricação de vidros. MSc. Dissertation. Escola Politécnica, Universidade de São Paulo, p. 106 (in portuguese).
- Dal Martello, E., Bernardis, S., Larseon, R.B., Tranel, G., Di Sabatino, M., Arnberg, L., 2011. Electrical fragmentation as a novel refining route for hydrothermal quartz for SoG-Si production. *Mineral. Eng.* 224, 209–216.
- Dhamrin, M., Saitoh, T., Kamisako, K., Yamada, K., Araki, N., Yamaga, I., et al., 2009. Technology development of high-quality n-type multicrystalline silicon for next-generation ultra-thin crystalline silicon solar cells. *Sol. Energy Mater. Sol. Cells* 93 (6–7), 1139–1142. <http://dx.doi.org/10.1016/j.solmat.2009.02.011>.
- Du, F., Li, J., Li, X., Zhang, Z., 2011. Improvement of iron removal from silica sand using ultrasound-assisted oxalic acid. *Ultrason. Sonochemistry* 18, 389–393.
- Fruth, M., Blankenburg, H.-J., 1992. Charakterisierung von authigenen idiomorphen Kohle- und Salinarquarzen durch Einschlussuntersuchungen. *Neues Jahrbuch Mineralogie. Abhandlungen* 165, 53–64 (in german).
- Fujiwara, E., Santos, M.F.M., Schenkel, E.A., Ono, E., Suzuki, C.K., 2015. Optical classification of quartz lumps by artificial neural networks. *Miner. Process. Extr. Metallurgy Rev.* 36, 281–287. <http://dx.doi.org/10.1080/08827508.2014.978315>.
- Goldstein, R.H., 2001. Fluid inclusions in sedimentary and diagenetic systems. *Lithos* 55, 159–193.
- Gao, B., Nakano, S., Kakimoto, K., 2011. Influence of reaction between silica crucible and graphite susceptor on impurities of multicrystalline silicon in a unidirectional solidification furnace. *J. Cryst. Growth* 314, 239–245.
- Götze, J., 2012. Mineralogy, geochemistry and cathodoluminescence of authigenic quartz from different sedimentary rocks. In: Götze, J., Möckel, R. (Eds.), *Quartz: Deposits, Mineralogy and Analytics*. Springer, Berlin, pp. 287–306.
- Götze, J., 2009. Chemistry, texture and physical properties of quartz – geological interpretation and technical application. *Mineral. Mag.* 73 (4), 645–671.
- Götze, J., Plötze, M., Graupner, T., Hallbauer, D.K., Bray, C.L., 2004. Trace element incorporation into quartz: a combined study by ICP-MS, electron spin resonance cathodoluminescence, capillary ion analysis, and gas chromatography. *Geochimica Cosmochimica Acta* 68 (18), 3741–3759.
- Götze, J., Plötze, M., Habermann, D., 2001. Origin, spectral characteristics and practical applications of the cathodoluminescence (CL) of quartz – a review. *Mineralogy Petrology* 71, 225–250.
- Griscom, D.L., 2006. Self-trapped holes in pure silica glass: a history of their discovery and characterization and an example of their critical significance to industry. *J. non-crystalline solids* 3512, 2601–2617.
- Haus, R., 2005. High demands on high purity. *Ind. Min.* 10, 62–67.
- Haus, R., Prinz, S., Priess, C., 2012. Assessment of high purity quartz resources. In: Götze, J., Möckel, R. (Eds.), *Quartz: Deposits, Mineralogy and Analytics*. Springer, Berlin, pp. 29–51.
- Huang, X., Kishi, H., Oishi, S., Watanabe, H., Sanpei, K., Sakai, S., Hoshikawa, K., 1999. Expansion behavior of bubbles in silica glass concerning czochralski (CZ) Si growth. *Jpn. J. Appl. Phys.* 38, 353–355.
- Iwasaki, H., Iwasaki, F., Oliveira, V.A.R., Hummel, D.C.A., Pasquali, M.A., Guzzo, P.L., Watanabe, N., Suzuki, C.K., 1991. Impurity content characterization of Brazilian quartz lumps. *J. J. Appl. Phys.* 30 (7), 1489–1495.
- Jiménez-López, C., Romanek, C.S., Huertas, F.J., Ohmoto, H., Caballero, E., 2004. Oxygen isotope fractionation in synthetic magnesian calcite. *Geochimica Cosmochimica Acta* 68 (16), 3367–3377.
- Karmann, I., 1987. O Grupo Rio Pardo (Proterozóico Médio e Superior): Uma Cobertura Paraplataformar da Margem Sudeste do Cráton do São Francisco. MSc. Dissertation. Instituto de Geociências, Universidade de São Paulo, p. 129 (in portuguese).
- Kelly, J.L., Fu, B., Kita, N.T., Valley, J.W., 2007. Optically continuous silcrete quartz cements of the St. peter sandstone: high precision oxygen isotope analysis by ion microscope. *Geochimica Cosmochimica Acta* 71, 3812–3832.
- Kempe, U., Götze, J., Dombon, E., Monecke, T., Poutivtsev, M., 2012. Quartz regeneration and its use as a repository of genetic information. In: Götze, J., Möckel, R. (Eds.), *Quartz: Deposits, Mineralogy and Analytics*. Springer, Berlin, pp. 331–355.
- Kempe, U., Götze, J., 2002. Cathodoluminescence (CL) behavior and crystal chemistry of apatite from rare-metal deposits. *Mineral. Mag.* 66 (1), 151–172.
- Kodama, M., Kishi, H., Kanda, M., Japan super quartz corp., 2010. Vitreous silica crucible for pulling silicon single crystal. US patent US2010/0251959.
- Krinsley, D.H., Doornkamp, J.C., 1973. Atlas of Quartz Sand Surface Textures. Cambridge University Press, Cambridge, p. 91.
- Kuzuu, N., Horikoshi, H., Nishimura, T., Kokubo, Y., 2003. Effects of heat treatment on absorption bands in OH-free and OH-containing fused quartz. *J. Apply. Phys.* 93, 9062–9071.
- Kvande, R., Arnberg, L., Martin, C., 2009. Influence of crucible and coating quality on the properties of multicrystalline silicon for solar cells. *J. Cryst. Growth* 311 (3), 765–768. <http://dx.doi.org/10.1016/j.jcrysgro.2008.09.152>.
- Le Ribeaault, L., 1977. L'exoscopie des quartz. Masson, Paris, p. 150 (in french).
- Lee, S.O., Tran, T., Park, Y.Y., Kim, M.J., 2006. Study on the kinetics of iron oxide leaching by oxalic acid. *Int. J. Miner. Process.* 80, 144–152.
- Li, J.-S., Li, X.-X., Shen, Q., Zhang, Z.-Z., Du, F.-H., 2010. Further purification of industrial quartz by much milder conditions and a harmless method. *Environ. Sci. Technol.* 44, 7673–7677.
- Liu, L.G., Gao, H.M., Zhang, L., 1996. Technical study on ore addressing for high-purity quartz sands. *Nonmet. Min.* 4 (4), 39–41.
- Loucaides, S., Van Cappellen, P., Roubeix, V., Moriceau, B., Ragueneau, O., 2012. Controls on the recycling and preservation of biogenic silica from biomineralization to burial. *Silicon* 4 (1), 7–22.
- Madhavaraju, J., Lee, Y.I., Armstrong-Altrin, J.S., Hussain, S.M., 2006. Microtextures on detrital quartz grain of upper Maastichtrian-Danian rocks of the cauvery Basin, Southeastern India: implications for provenance and depositional environments. *Geosciences J.* 10 (1), 23–34.
- Mahaney, W.C., 2002. Atlas of Sand Grain Surface Texture and Applications. Oxford University Press, New York, p. 237.
- Minami, T., Maeda, S., Higasa, M., Kashima, K., 2011. In-situ observation of bubble formation at silicon melt-silica glass interface. *J. Cryst. Growth* 318, 196–199.
- Moore, P., 2005. High-purity quartz. *Ind. Min.* 455, 53–57 (August).
- Müller, A., Wanvik, J.E., Ihlen, R.M., 2012. Petrological and chemical characterization of high-purity quartz deposits with examples from Norway. In: Götze, J., Möckel, R. (Eds.), *Quartz: Deposits, Mineralogy and Analytics*. Springer, Berlin, pp. 71–118.
- Müller, A., Koch-Müller, M., 2009. Hydrogen speciation and trace element contents of igneous, hydrothermal and metamorphic quartz from Norway. *Mineral. Mag.* 73, 569–583.
- Müller, A., Ihlen, P.M., Wanvik, J.E., Flem, B., 2007. High-purity quartz mineralization in kyanite quartzites, Norway. *Min. Deposita* 42, 523–533.
- Müller, A., Wiedenbeck, M., van den Kerkhof, A.M., Kronz, A., Simon, K., 2003. Trace elements in quartz – a combined electron microprobe, secondary ion mass spectrometry, laser-ablation ICP-MS, and cathodoluminescence study. *Eur. J. Mineral.* 15, 747–763.
- Pedreira, A.J., 1999. Evolução Sedimentar e Tectônica da Bacia Metasedimentar do Rio Pardo: Uma Síntese. *Rev. Bras. Geociências* 29 (3), 339–344 (in portuguese).
- Rakov, L.T., 2006. Mechanisms of isomorphous substitution in quartz. *Geochem. Int.* 44 (10), 1004–1014.
- Romanelli, M., Di Benedetto, F., Bartali, L., Innocenti, M., Fornaciai, G., Montegrossi, G., Pardi, L.A., Zoleo, A., Capacci, F., 2012. ESEEM of industrial quartz powders: insights into crystal chemistry of Al defects. *Phys. Chem. Miner.* 39, 479–490. <http://dx.doi.org/10.1007/s00269-012-0502-3>.
- Ruiz, M.S., Cabral Junior, M., Tanno, L.C., Coelho, J.M., Cortés, P.L., 2013. Desafios e perspectivas da produção de areia industrial. *Holos* 29 (5), 50–68 (in portuguese).
- Santos, M.F.M., Fujiwara, E., Schenkel, E.A., Enzweiler, J., Suzuki, C.K., 2015. Processing of quartz lumps rejected by the silicone industry to obtain a raw material for silica glass. *I. J. Mineral. Process.* 135, 65–70.
- Santos, M.F.M., Fujiwara, E., Schenkel, E.A., Enzweiler, J., Suzuki, C.K., 2014. Quartz resources in the Serra de Santa Helena formation, Brazil: a geochemical and technological study. *J. South Am. Earth Sci.* 56, 328–338.
- Santos, M.F.M., Fujiwara, E., De Paula, F.D., Suzuki, C.K., 2013. Opacity measurements on quartz and its influence on silica glass properties. *I. J. Mineral. Process.* 124, 141–144.
- Schmidt, M., Xeflide, S., Botz, R., Mann, 2005. Oxygen isotope fractionation during synthesis of CaMg-carbonate and implications for sedimentary dolomite formation. *Geochimica Cosmochimica Acta* 68 (19), 4665–4674.
- Schreiber, A., Kühn, B., Arnold, E., Schilling, F.-J., Witzke, H.-D., 2005. Radiation resistance of quartz glass for VUV discharge lamps. *J. Phys. D: App. Phys.* 38, 3242–3250.
- Schieber, J., Krinsley, D., Riciputi, L., 2000. Diagenetic origin of quartz silt in mudstones and implications for silica cycling. *Nature* 406, 981–984.
- Schrön, W., Bauman, L., Rank, K., 1982. Zur Charakterisierung von Quarzgenerationen in den postmagmatogenen Ertzformationen des Erzgebirges. *Zeitschrift für Geol. Wiss.* 16, 229–244 (in german).
- Schultz, P.C., 1974. Optical absorption of the elements in vitreous silica. *J. Am. Ceram. Soc.* 57, 309–313.
- Suzuki, C.K., Santos, M.F.M., Ono, E., Fujiwara, E., 2012. Strategic high quality quartz supply for fusion into silica glass. In: Varshneya, A.K., Schaeffer, H.A., Richardson, K.A., Wightman, M., Pye, D. (Eds.), *Processing Properties and Applications of Glass and Optical Materials: Ceramic Transactions*. The American Ceramic Society, pp. 69–74.
- Teixeira, W., Kamo, S.L., Arcanjo, J.B.A., 1997. U-pb and baddelyite age and tectonic interpretation of the Itabuna Alkaline suite, São Francisco Craton, Brazil. *J. South Am. Earth Sci.* 10 (1), 91–98.
- Torikai, D., 1994. Preparação e caracterização de sílica vítrea de alta pureza por Verneuil: a partir de sílica sol-gel. Dissertation. Campinas State University (in portuguese).
- Ubalindi, S., Piga, L., Fornari, P., Massidda, R., 1996. Removal of iron from quartz sands: a study by column leaching using a complete factorial design. *Hydro-metallurgy* 40, 369–379.
- Van den Kerkhof, A.M., Hein, U.F., 2001. Fluid inclusion petrography. *Lithos* 55, 27–47.
- Vos, K., Vandenberghe, N., Elsen, J., 2014. Surface textural analysis of quartz grains by scanning electron microscopy (SEM): from sample preparation to environmental interpretation. *Earth-Science Rev.* 128, 93–104.
- Wait, I.W., Johnston, C.T., Blatchley, E.R., 2007. The influence of oxidation reduction potential and water treatment process on quartz lamp sleeves fouling in ultraviolet disinfection reactors. *Water Res.* 41, 2427–2436.
- Waugh, B., 1970. Formation of quartz overgrowths in the penrith sandstone (lower Permian) of northwest England as revealed by scanning electron microscopy. *Sedimentology* 14, 309–320.
- Yahamara, K., Huang, X., Sakai, S., Utsonomiya, A., Tsurita, Y., Hoshikawa, K., 2001. Surface of silica glass reacting with silicon melt: effect of raw materials for silica crucibles. *Jpn. J. Appl. Phys.* 40, 1178–1182.